reference to the summed PET and CT images. MBF was calculated using the one-tissue compartment model developed by DeGrado et al. with PMOD software.[6] Global and regional MBF (basal, mid, apical segments) were used for the evaluations.[7] CFR was expressed as the ratio of MBF during stress to MBF at rest. Change in CFR was evaluated as the ratio of post-treatment to pre-treatment CFR. Normal male SD rats (n=6, 10-11 weeks old, BW: 369-429 g) were used for the validation study for quantitative PET measurements with a stress agent.

Assessment of Cardiac Function

The cardiac function was evaluated by echocardiography 2 and 4 weeks after each treatment (n=11 for each group) **(Figure 6)**. Baseline measurements were made before each treatment. Transthoracic echocardiography was performed with using a SONOS 5500 (Philips Electronics, Tokyo, Japan) equipped with a 12-MHz annular array transducer under general anaesthesia induced and maintained by inhalation of isoflurane (2%, 0.2 mL/min) as mentioned above **(Figure 1)**. The hearts were imaged in short-axis 2D views at the level of the papillary muscles, and the LV end-systolic and end-diastolic dimensions were determined. LV ejection fraction was calculated by Pombo's method.

LV pressure-volume loop analysis with cardiac catheterization was performed for each group as previously described.[1] In brief, a median sternotomy was performed and the LV apex was carefully dissected to minimize hemorrhaging. A MicroTip catheter transducer (SPR-671; Millar Instruments, Inc, Houston, Tex) and conductance catheter (Unique Medical Co, Tokyo, Japan) were then placed longitudinally into the left ventricle from the apex. LV pressure-volume relationships were determined by transiently compressing the inferior vena cava.

Exercise Tolerance

Eleven rats in each group were acclimated to a rodent activity wheel (MULTI-FUNCTIONAL ACTIVITY WHEEL, MK-770M, Muromachi, Tokyo, Japan) by running daily for 5 days. During the acclimation period, the round speed was increased from 5 to 10 rpm, with the exercise duration maintained at 20 minutes. On the day of tolerance testing, animals were placed on the activity wheel at round speeds of 4 or 8 rpm and allowed to exercise until fatigue. Fatigue was defined as the point at which the animal failed to keep pace with the activity wheel despite constant physical prodding for 1 minute. Running distance was used as an index of maximal capacity for exercise.

Communication Between Pedicle Omentum and Native Coronary Artery

Communication between the coronary arteries and branches of the gastroepiploic artery in the OM specimens was evaluated using 3 different methods in a different series of OM-only and combined group (n=12 for each group) **(Figure 7)**.

Aortic Root Angiography using Barium Sulfate

We performed a postmortem angiography examination from the aortic root to verify antegrade flow from the OM into the heart (n=4 for each). In brief, a catheter with an internal diameter of 0.89 mm (COVIDIEN Ltd, Tokyo, Japan) was inserted from the right carotid artery into the aortic root, followed by systemic heparinization (1000 IU heparin). The rats were euthanized with an overdose of pentobarbital, then an incision was made in the right jugular vein and lactated Ringer's solution was manually perfused through the cannula for 5 minutes. Approximately 3 mL of a solution consisting of 70% weight/volume barium sulfate

suspended in 7% gelatin was then injected in a retrograde manner via the catheter using a programmed syringe pump. Angiograms were obtained with a angiographic system (MFX-80HK, Hitex) consisting of an open type 1-μm microfocus X ray source (L9191, Hamamatsu Photonics) and a 50/100 mm (2"/4") dual mode X-ray image intensifier (E5877JCD1-2N, Toshiba) set at 60 kV and 60 μA.

Selective India Ink Perfusion via Celiac Artery

Next, we selectively injected India ink into the celiac artery to visually and histologically confirm vessel communication between the pedicle OM and native coronary artery (n=4 for each). The catheter was inserted via the abdominal aorta and its tip placed near the celiac artery, followed by systemic heparinization. The chest was reopened to expose the wrapped heart, taking care to avoid injuring the OM. The heart was harvested after perfusion fixation of the vasculature, as described above. We ligated the abdominal aorta just proximal from the tip of the catheter in advance and selectively injected India ink via the celiac artery into the heart, and then performed histological analysis.

Selective Perfusion via Aortic Root and Celiac Artery Using Two Different MICROFIL Colors

A catheter was inserted from the right carotid artery into the aortic root and another was inserted from the abdominal aorta into the celiac artery, followed by systemic heparinization (1000 IU heparin). After perfusion fixation, we ligated the abdominal aorta just proximal from the tip of the catheter. Approximately 3 mL of 2 different colors of MICROFIL solution (MICROFIL Silicone Rubber Injection Compounds, Flow Tech, Inc.) was injected in an antegrade manner into the celiac arterial trunk (MV-120 Blue) and a retrograde manner from

the aortic root into the coronary artery (MV-117 Orange). The solution was allowed to solidify for more than 30 minutes. The heart and OM were removed en bloc, and placed in 10% neutral buffered formalin for several days. The tissue was then cleared using sequential 24-hour incubations in 25% ethanol, 50% ethanol, 75% ethanol, 95% ethanol, 100% ethanol, and methylsalicylate, according to the manufacturer's instructions. Evidence of vessel communication between the native coronary artery and OM-flap was photographed in multiple planes using an Olympus DP70 camera attached to an Olympus SZX 12 stereo microscope (Olympus, Tokyo, Japan).

Creation of Surgically Joined Parabiotic Pairs Model

To further confirm whether the OM- and host myocardium-derived endothelial cells migrated toward the cell-sheet, we established two types of parabiotic pair models (n=4 for each) **(Figure 8)**. To determine whether OM-derived endothelial cells migrated toward the cell-sheet, the parabiotic pairs model were established by producing wild-type MI model rats (recipient) to receive transplantation of wild-type oriented cell-sheets which was labeled with Cell Tracker TM Orange CMTMR (Invitrogen, Oregon, USA), followed by coverage with a pedicle OM derived from a transgenic ubiquitously expressing GFP rat (donor) and then surgically joining them. Similarly, to determine whether host myocardium-derived endothelial cells migrated toward the cell-sheet, we also established another parabiotic pairs model by producing GFP-transgenic MI model rats (recipient) to receive transplantation of wild-type oriented cell-sheets which was labeled with Cell Tracker TM Orange CMTMR, followed by coverage with a pedicle OM derived from a wild-type rat (donor) and then surgically joining them.

Parabiotic pair rats were anaesthetized by inhalation of isoflurane (2%, 0.2 mL/min) and

maintained for 72 hours under mechanical ventilation with a continuous infusion of 5% glucose (0.3 ml/h), then subjected to histological analyses.

In vitro Migration assay

To investigate cell migration in response to skeletal myoblast cells cultured in conditioned medium, a modified Boyden chamber migration assay was performed using an HTS FluoroBlok™ Multiwell Insert System (BD Falcon, NJ, USA) containing filters with a pore size of 8 μm. Briefly, human umbilical vein endothelial cells (HUVECs) (purchased from Lonza) were grown in EGM-2 culture medium (Lonza, Walkersville, USA). To visualize them, HUVECs were stained in advance with Cell Tracker TM Orange CMTMR (Invitrogen, Oregon, USA). A suspension of 5×10^4 HUVECs in HUVEC-cultured medium (350 μm) was applied to each upper chamber. The lower chamber was filled with 1.0 ml of concentrated skeletal myoblasts-cultured supernatant composed of DMEM with 20% fetal bovine serum (100% conditioned medium), 10-fold diluted conditioned medium (10% conditioned medium) or DMEM, and 20% fetal bovine serum (control group). After incubation at 37°C for 2 hours, the number of migrated cells was counted in 15 randomly chosen fields under 100×magnification using fluorescence microscopy (BIOREVO BZ-9000, KEYENCE, Osaka, Japan). Two replicate samples were used in each experiment, which were performed at least twice. Migrating cells were analyzed using a light microscope and reported as numbers of migrating cells per mm^2.

Statistical analysis

Data are expressed as the mean ± SEM unless otherwise stated. Student's t test (2 tailed) was used to compare 2 groups of independent samples. One-way and two-way ANOVA with

Bonferroni correction for repeated measures were performed to assess within and between group differences following the treatments. Following ANOVA, between group comparisons were made using a Student's t-test (2-tailed). Multiplicity in pairwise comparisons was corrected by the Bonferroni procedure. The Statistical Package Software System (SPSS v15, SPSS Inc, Chicago, USA) and JMP 9.0 (SAS Institute Inc, Cary, NC) were used for all analyses, with P values <0.05 deemed to indicate significance.

References

1. Sekiya N, Matsumiya G, Miyagawa S, Saito A, Shimizu T, Okano T, Kawaguchi N, Matsuura N, Sawa Y. Layered transplantation of myoblast sheets attenuates adverse cardiac remodeling of the infarcted heart. *J Thorac Cardiovasc Surg* 2009;**138**:985-993.
2. Mancuso MR, Davis R, Norberg SM, O'Brien S, Sennino B, Nakahara T, Yao VJ, Inai T, Brooks P, Freimark B, Shalinsky DR, Hu-Lowe DD, McDonald DM. Rapid vascular regrowth in tumors after reversal of VEGF inhibition. *J Clin Invest* 2006;**116**:2610-2621.
3. Jenkins MJ, Edgley AJ, Sonobe T, Umetani K, Schwenke DO, Fujii Y, Brown RD, Kelly DJ, Shirai M, Pearson JT. Dynamic synchrotron imaging of diabetic rat coronary microcirculation in vivo. *Arterioscler Thromb Vasc Biol* 2012;**32**:370-377.
4. Ludmer PL, Selwyn AP, Shook TL, Wayne RR, Mudge GH, Alexander RW, Ganz P. Paradoxical vasoconstriction induced by acetylcholine in atherosclerotic coronary arteries. *N Engl J Med* 1986;**315**:1046-1051
5. Croteau E, Bénard F, Bentourkia M, Rousseau J, Paquette M, Lecomte R. Quantitative myocardial perfusion and coronary reserve in rats with 13N-ammonia and small animal PET: impact of anesthesia and pharmacologic stress agents. *J Nucl Med* 2004;**45**:1924-1930.
6. DeGrado TR, Hanson MW, Turkington TG, Delong DM, Brezinski DA, Vallée JP, Hedlund LW, Zhang J, Cobb F, Sullivan MJ, Coleman RE. Estimation of myocardial blood flow for longitudinal studies with 13N-labeled ammonia and positron emission tomography. *Med J Nucl Cardiol* 1996;**3**:494-507.
7. Cerqueira MD, Weissman NJ, Dilsizian V, Jacobs AK, Kaul S, Laskey WK, Pennell DJ, Rumberger JA, Ryan T, Verani MS; American Heart Association Writing Group on Myocardial Segmentation and Registration for Cardiac Imaging. Standardized myocardial

segmentation and nomenclature for tomographic imaging of the heart. A statement for healthcare professionals from the Cardiac Imaging Committee of the Council on Clinical Cardiology of the American Heart Association. *Circulation* 2002:**29**;105:539-542.

TISSUE ENGINEERING: Part A
Volume 20, Numbers 3 and 4, 2014

DOI: 10.1089/ten.tea.2012.0534

Addition of Mesenchymal Stem Cells Enhances the Therapeutic Effects of Skeletal Myoblast Cell-Sheet Transplantation in a Rat Ischemic Cardiomyopathy Model

Yasuhiro Shudo, MD,[1] Shigeru Miyagawa, MD, PhD,[1] Hanayuki Ohkura, PhD,[1,2] Satsuki Fukushima, MD, PhD,[1] Atsuhiro Saito, PhD,[1] Motoko Shiozaki, PhD,[1] Naomasa Kawaguchi, PhD,[3] Nariaki Matsuura, MD, PhD,[3] Tatsuya Shimizu, MD, PhD,[4] Teruo Okano, PhD,[4] Akifumi Matsuyama, MD, PhD,[2] and Yoshiki Sawa, MD, PhD[1]

Introduction: Functional skeletal myoblasts (SMBs) are transplanted into the heart effectively and safely as cell sheets, which induce functional recovery in myocardial infarction (MI) patients without lethal arrhythmia. However, their therapeutic effect is limited by ischemia. Mesenchymal stem cells (MSCs) have prosurvival/proliferation and antiapoptotic effects on co-cultured cells *in vitro*. We hypothesized that adding MSCs to the SMB cell sheets might enhance SMB survival post-transplantation and improve their therapeutic effects.
Methods and Results: Cell sheets of primary SMBs of male Lewis rats (r-SMBs), primary MSCs of human female fat tissues (h-MSCs), and their co-cultures were generated using temperature-responsive dishes. The levels of candidate paracrine factors, rat hepatocyte growth factor and vascular endothelial growth factor, *in vitro* were significantly greater in the h-MSC/r-SMB co-cultures than in those containing r-SMBs only, by real-time PCR and enzyme-linked immunosorbent assay (ELISA). MI was generated by left-coronary artery occlusion in female athymic nude rats. Two weeks later, co-cultured r-SMB or h-MSC cell sheets were implanted or no treatment was performed ($n=10$ each). Eight weeks later, systolic and diastolic function parameters were improved in all three treatment groups compared to no treatment, with the greatest improvement in the co-cultured cell sheet transplantation group. Consistent results were found for capillary density, collagen accumulation, myocyte hypertrophy, Akt-signaling, STAT3 signaling, and survival of transplanted cells of rat origin, and were related to poly (ADP-ribose) polymerase-dependent signal transduction.
Conclusions: Adding MSCs to SMB cell sheets enhanced the sheets' angiogenesis-related paracrine mechanics and, consequently, functional recovery in a rat MI model, suggesting a possible strategy for clinical applications.

Introduction

A RECENT LARGE-SCALE clinical trial, in which autologous skeletal myoblasts (SMBs) were directly injected into the heart by needle, reported only modest therapeutic benefits and a substantial risk of ventricular arrhythmias, due at least partly to the delivery method.[1,2] The major drawbacks of SMB delivery by needle injection are poor cell survival in the heart, leading to insufficient paracrine effects, and mechanical myocardial injury, potentially causing lethal arrhythmia.[1–3] In contrast, cell-sheet techniques, which we developed, deliver SMBs more effectively with minimal myocardial injury, enhanced paracrine effects, and consequently better cardiac function than attained by needle injection.[4–8]

The mechanism by which damaged myocardium is restored by transplanted SMB cell sheets is complex, involving many pathways.[4–8] Recent reports show beneficial effects of SMB cell-sheet transplantation in several animal experimental models and patients with heart failure, which are primarily attributed to cytokine secretion from the transplanted cell sheets (i.e., a paracrine effect).[4–9]

However, SMB cell sheets attached to the surface of the infarcted myocardium are poorly supported by the vascular

Presented at the American Heart Association, Orlando, Florida, November 12–15, 2011.
[1]Department of Cardiovascular Surgery, Osaka University Graduate School of Medicine, Suita, Japan.
[2]Laboratory for Somatic Stem Cell Therapy, Foundation of Biomedical Research and Innovation, Kobe, Japan.
[3]Department of Pathology, Osaka University Graduate School of Medicine, Suita, Japan.
[4]Institute of Advanced Biomedical Engineering and Science, Tokyo Women's Medical University, Tokyo, Japan.

network of the native myocardium, which limits the survival of the SMBs and, consequently, their therapeutic effects.[7] Thus, conventional SMB cell-sheet transplantation might be insufficient to repair severely damaged myocardium, which has poor viability. Mesenchymal stem cells (MSCs) are used as feeder cells to support the survival, proliferation, and differentiation of co-cultured stem/progenitor cells *in vitro*.[10–12] Moreover, MSCs are advantageous for cellular therapy because they are multipotent, potentially immune privileged, and expand easily *ex vivo*. MSCs also proliferate rapidly and induce angiogenesis.[13,14]

We hypothesized that adding MSCs to the SMB cell sheets *in vitro* might enhance their survival and function after transplantation, which might enhance the benefits of SMB cell-sheet transplantation therapy. Here, we investigated whether co-culturing SMBs with MSCs would enhance the SMBs' cytokine production *in vitro*. We also examined the therapeutic effects on chronic ischemic heart failure of transplanting cell sheets created from co-cultured SMBs and MSCs, compared with SMB-only and MSC-only cell sheets.

Materials and Methods

This study was approved by the Institutional Ethics Committee of the Osaka University. Humane animal care was used in compliance with the "Principles of Laboratory Animal Care" formulated by the National Society for Medical Research, and the "Guide for the Care and Use of Laboratory Animals" prepared by the Institute of Animal Resources and published by the National Institutes of Health (Publication No. 85–23, revised 1996). All procedures and evaluations, including assessments of cardiac parameters, were carried out in a blinded manner. The authors had full access to the data and take full responsibility for its integrity. All authors have read and agreed to the article as written.

Isolation of SMBs and adipose tissue-derived mesenchymal cells, and cell-sheet preparation

Primary skeletal myoblasts of rat origin (r-SMBs) were isolated from Lewis rats (3 weeks old, male; CLEA Japan, Inc.) and expanded *in vitro* as described previously[7,8]: more than 70% of the isolated cells were actin positive and 60–70% were desmin positive, as determined by flow cytometry (data not shown). To detect r-SMBs, we used GFP transgenic Lewis rats.[15] Primary human MSCs (h-MSCs) were isolated from female subcutaneous adipose tissue samples as described.[12] h-MSCs exhibit mesenchymal morphology (Fig. 1A). Cell sheets consisting of r-SMBs or h-MSCs were prepared using temperature-responsive culture dishes (UpCell®; CellSeed), as described.[12] Cell sheets containing both r-SMBs and h-MSCs were prepared by co-culturing these cells in temperature-responsive culture dishes.

Rat myocardial infarction model and cell-sheet implantation

A proximal site of the left anterior descending coronary artery (LCA) of athymic nude rats (F344/NJcl-rnu/rnu, 8-week-old, female, 120–130 g; CLEA Japan) was permanently occluded using a thoracotomy approach. The animals were then kept in temperature-controlled individual cages for 2 weeks to generate a subacute ischemic heart failure model.[7,8,12] The rats were then divided into 4 experimental groups ($n=10$ in each) as follows: (1) transplantation of triple-layer h-MSC cell sheets (7.5×10^5 cells per sheet), (2) transplantation of triple-layer r-SMB cell sheets (3.0×10^6 cells per sheet), (3) transplantation of triple-layer co-cultured r-SMB (3.0×10^6 cells per sheet) and h-MSC (7.5×10^5 cells per sheet) sheets, and (4) no treatment (control) (Fig. 1B). Thereafter, the rats were kept in individual cages for 4 weeks.

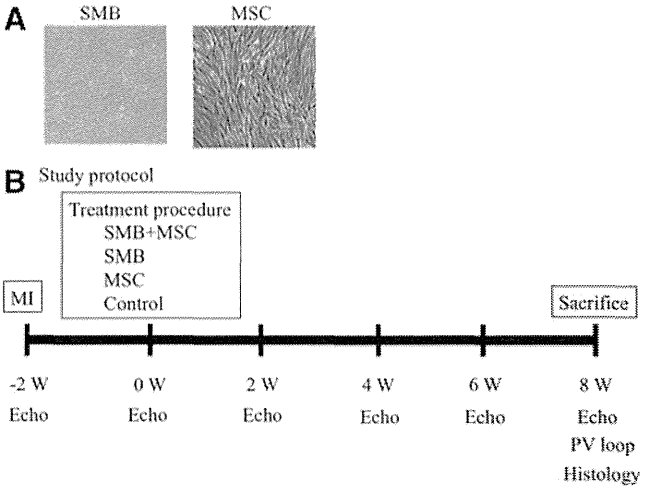

FIG. 1. **(A)** Morphology of SMB and MSC. **(B)** Study protocol used for the assessment of cardiac function and histology. Athymic nude rats (F344/NJcl-rnu/rnu) underwent induction of myocardial infarction by occluding the LAD permanently, followed by the treatment procedure 2 weeks later. Cardiac function was assessed by echocardiography just before 2, 4, 6, and 8 weeks after the treatment procedure. Eight weeks after the treatment procedure, invasive hemodynamic analysis and histological examination were performed following the sacrifice. SMB+MSC, co-culture of SMBs and MSCs; SMB, skeletal myoblast; MSC, derived mesenchymal stem cell; Echo, echocardiography; PV loop, invasive hemodynamic analysis. Color images available online at www.liebertpub.com/tea

Echocardiography

Echocardiography was performed under general anesthesia using 1% isoflurane just before, and 2, 4, 6, and 8 weeks after the treatment procedure (SONOS 7500; Philips Medical Systems) (Fig. 1B). Left ventricular end-diastolic diameter (LVEDD), left ventricular end-systolic diameter (LVESD), and end diastolic anterior wall thickness at the level of the papillary muscles were measured for at least three consecutive cardiac cycles, following the American Society for Echocardiology leading-edge method. Fractional shortening (FS) and ejection fraction (EF) were calculated as parameters of systolic function, as follows:

$$FS\ (\%) = (LVEDD - LVESD)/LVEDD$$

$$EF\ (\%) = [(LVEDD^3 - LVESD^3)/LVEDD^3].^4$$

Cardiac catheterization

To assess systolic and diastolic cardiac function, cardiac catheterization was performed under general anesthesia using 1% isoflurane, 8 weeks after the treatment procedure. A MicroTip catheter transducer (SPR-671; Millar Instruments, Inc.) and conductance catheters (Unique Medical

Co.) were placed longitudinally in the left ventricle (LV) from the apex and connected to an Integral 3-signal conditioner-processor (Unique Medical Co.). End-systolic pressure-volume relationships (ESPVR) were determined by transiently compressing the inferior vena cava. Data were recorded as a series of pressure–volume loops (~20), which were analyzed using Integral 3 software (Unique Medical Co.). The maximal and minimal rates of change in LV pressure (dP/dt max and dP/dt min, respectively) were obtained from steady-state beats using custom-made software. We assessed the early active part of the relaxation using the relaxation time constant (τ), which was determined from the LV pressure decay curve. After the hemodynamic assessment, the heart was removed for further biochemical and histological analyses.

Real-time quantitative PCR

Total RNA was extracted from cultured cell sheets or cardiac muscle tissue 8 weeks post-transplantation using TRIzol reagent (Invitrogen) and reverse transcribed into cDNA using TaqMan Reverse Transcription Reagents (Applied Biosystems). Subsequently, real-time PCR assays were performed using an ABI PRISM 7700 machine.[4,7,8] Hepatocyte growth factor (HGF), vascular endothelial growth factor (VEGF), basic fibroblast growth factor (bFGF), insulin growth factor (IGF), and thymosin β were assayed using rat-specific primers and probes (Applied Biosystems). The average copy number of gene transcripts for each sample was normalized to that for GAPDH.

Survival of grafted donor cells

The presence of grafted male cells in the female heart was quantitatively assessed by real-time PCR for the Y chromosome-specific gene *sry*. Four weeks after cell-sheet transplantation, genomic DNA was extracted from the entire LV walls using the QIAmp genomic DNA purification system (Qiagen). The signals for the autosomal single-copy gene were normalized to the amount of total DNA.[7] The primers were *sry*: forward, 5′ GCCTCAGGACATATTAATCTCTGGAG-3′; reverse, 5′-GCTGATCTCTGAATTCTGCATGC-3′.

Protein analysis

Enzyme-linked immunosorbent assay (ELISA) kits were used to measure proteins, such as HGF (Institute of Immunology) and VEGF (Quantikine; R&D) of rat origin, secreted from the cultured cell sheets *in vitro*, according to the manufacturers' suggested protocols. Values were calibrated for the extracted total proteins ($n=5$ in each group). The ELISA kits were also used to quantitatively analyze HGF (r-HGF) and VEGF (r-VEGF) of rat origin in heart tissue lysates ($n=5$ in each group).

Cytokine/chemokine multiplex immunology assay

The amount of each protein secreted from the cultured cell sheets *in vitro* was measured by Milliplex Rat Cytokine/Chemokine Panel Premixed 32Plex (Millipore), according to the manufacturer's instructions.[4] In this procedure, we applied human SMBs (h-SMBs) isolated and cultured from the patient (age 53 years, male) and expand *in vitro* as described previously.[6]

Histological analyses

Eight weeks after cell-sheet implantation, the hearts were dissected, fixed in 4% paraformaldehyde, and embedded in either optimum cutting temperature compound for 5-μm-thick cryosections or paraffin for 5-μm-thick sections ($n=5$ in each group) (Fig. 1). The paraffin-embedded sections were used for routine hematoxylin–eosin (HE) staining to assess the myocardial structure. Masson's trichrome staining was performed to assess cardiac fibrosis in the remote myocardium. The fibrotic cardiac area was calculated as the percentage of myocardial area. The data were collected from 10 individual views per heart at a magnification of ×200. The heart sections were also stained with an antibody to von Willebrand Factor (vWF) to assess capillary density, which was calculated as the number of positively stained capillary vessels that were 5–10 μm in diameter in 10 randomly selected fields in the peri-infarct area, per heart. To determine the extent of apoptosis, sections from frozen tissue samples were subjected to terminal deoxynucleotidyl transferase-mediated dUTP nick end labeling (TUNEL) with an *in situ* apoptosis detection kit (Apoptag; Chemicon). Image J software was used for quantitative morphometric analysis.

To detect r-SMBs, we used GFP transgenic Lewis rats.[15] Cryosections were stained with an anti-HGF antibody (1:50 dilution; LifeSpan BioSciences). To detect h-MSCs and differentiation of the transplanted cell sheet, sections were stained with an antibody to human leukocyte antigen (1:50 dilution; Dako). The secondary antibody was Alexa Fluor 555 goat anti-mouse (1:200 dilution; Molecular Probes). Cell nuclei were counterstained with 6-diamidino-2-phenylindole (DAPI; Invitrogen). The images were examined by fluorescence microscopy (Keyence).

Western blotting

Tissue homogenates from LV samples in the cell-sheet transplanted site ($n=3$ in each group, on day 1) were prepared using lysis buffer (100 mM Tris pH 7.4, 20% SDS, 10 mM EDTA. 10 mM NaF, 2 mM sodium orthovanadate). The equivalent total protein was loaded onto SDS-polyacrylamide gel electrophoresis gels. Antibodies obtained from Cell Signaling were antiphosphorylated STAT3 (#9145), antiphosphorylated Akt (#4051), anti-Bcl_2 (#2876), and anti-poly (ADP-ribose) polymerase (PARP) (#9542). The labeled membrane was stripped and then re-probed with anti-STAT3 (#9132), anti-AKT (#9272), and anti-cleaved PARP (#9545) antibodies. Blots were scanned, and quantitative analysis was performed using Image J software. The relative proportion of the phosphorylated STAT3 was referred to that of the STAT3. The relative proportion of the phosphorylated Akt was referred to that of the Akt. The relative proportion of the PARP, cleaved PARP, Bcl_2 was referred to that of the control group.

Statistical analysis

Continuous variables are expressed as the mean ± SD. The significance of differences was determined using a two-tailed multiple *t*-test with Bonferroni correction following repeated-measures analysis of variance for individual differences. A *p*-value less than 0.05 was considered to be statistically significant. All statistical calculations were performed using the SPSS software (version 11.0; SPSS, Inc.).

Results

Production and release of cytokines/chemokines by cell sheets

Both h-SMBs and h-MSCs, as analyzed by cytokine antibody array, released abundant angiogenic factors *in vitro*, with distance profiles (Fig. 2A). Co-cultures of h-SMBs and h-MSCs showed significantly enhanced levels of HGF, VEGF, Leptin, and PECAM-1, but not of follistatin, G-CSF, IL-8, or PDGF-BB from the h-SMBs.

The seeding ratio of 4:1 r-SMBs:h-MSCs elicited the greatest *in vitro* mRNA expression of rat HGF and VEGF by real-time PCR (Fig. 2B). The mRNA levels of SMB-derived r-HGF and r-VEGF, analyzed by real-time PCR using rat-specific primers, were significantly greater in the co-cultured cell sheets than r-SMB-only ones (Fig. 2C), whereas the mRNA levels of IGF-1, bFGF, SDF-1, and TMSB4 were essentially the same (Supplementary Fig. S1; Supplementary Data are available online at www.liebertpub.com/tea). No mRNAs for cytokines of rat origin were detected in h-MSC-only cell sheets. Rat HGF and VEGF in the culture supernatants, analyzed by ELISA with rat-specific primary antibodies, were significantly higher in the co-culture supernatants than the r-SMB-only ones, and no rat cytokines were detected in the h-MSC-only supernatants (Fig. 2D).

Cardiac functional recovery after cell-sheet transplantation

The effects of cell-sheet transplantation on cardiac function were assessed in a rat chronic ischemic heart-failure model. Two weeks after permanent occlusion of the LCA, the LV developed echocardiographic features typical of chronic ischemic heart failure, including decreased FS, EF, and anterior wall thickness, and increased end-diastolic and systolic diameter (EDD and ESD, respectively). Following myocardial

A Cytokine/Chemokine multiplex immunology assay

	SMB+MSC	SMB	MSC	Medium only
Follistatin (pg/ml)	276±35*,†	350±56†	127±8.0	3.3
G-CSF (pg/ml)	333±44*,†	487±89†	7.7±0.7	1
HGF (pg/ml)	1190±256*,†	167±28†	695±44	3.8
IL-8 (pg/ml)	805±36*,†	1079±138†	579±29	0.6
Leptin (pg/ml)	1335±690*,†	262±40	195±13	59
PDGF-BB (pg/ml)	51±11*	25±2†	51±3	3.3
PECAM-1 (pg/ml)	438±70*	239±71†	386±16	64
VEGF (pg/ml)	5673±812*,†	1402±272	2019±184	1.9

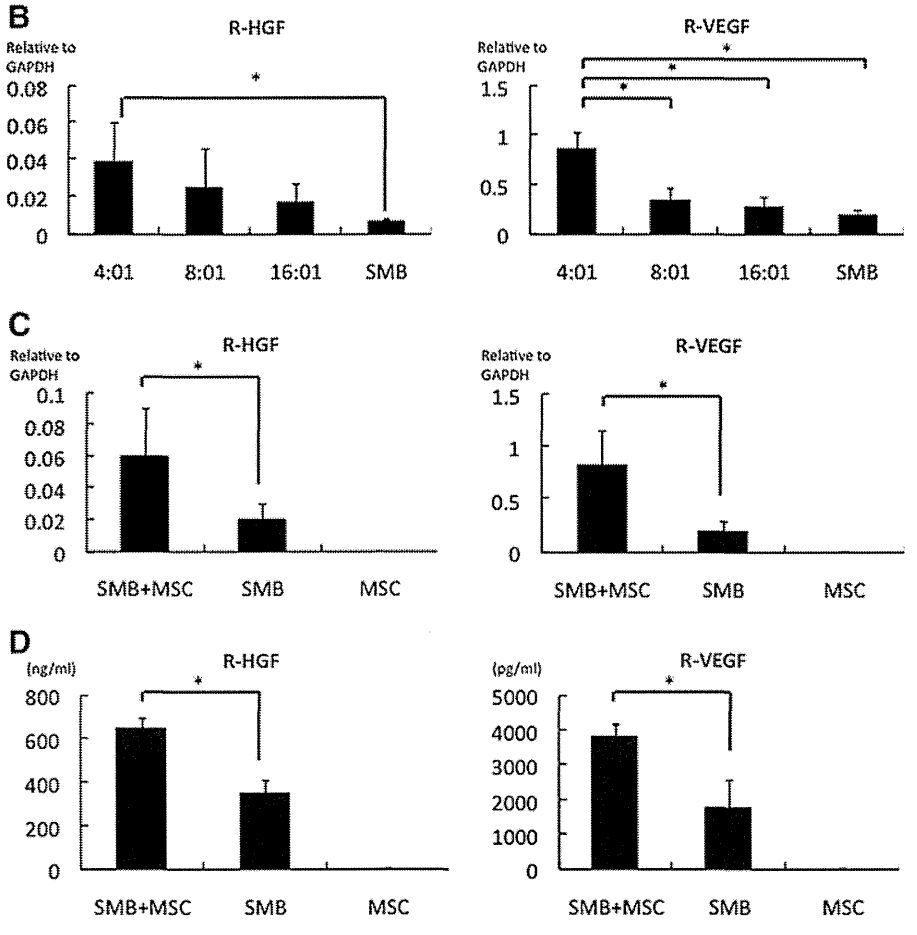

FIG. 2. Production and release of angiogenic factors by cell sheets. **(A)** Cytokine/chemokine multiplex immunology assay results from cultured cell sheets *in vitro*, prepared from human SMBs, human MSCs (h-MSCs), or both. SMB+MSC showed significantly enhanced the release of HGF, VEGF, leptin, and PECAM-1. $N=4$ in each group. $^{*}p<0.05$ versus SMB. $^{\dagger}p<0.05$ versus MSC. **(B)** Optimal seeding ratio of rat SMBs (r-SMBs) to h-MSCs. The *in vitro* mRNA levels of rat HGF and VEGF, analyzed by real-time PCR, were highest at 4:1 r-SMBs:h-MSCs. $N=4$ in each group. $^{*}p<0.05$. **(C)** mRNA levels in cultured cell sheets determined by real-time PCR using rat-specific primers. The SMB+MSC sheets expressed significantly more HGF and VEGF than the SMB-only ones. $N=5$ in each group. $^{*}p<0.05$. **(D)** Secretion of cytokines into the culture medium determined by enzyme-linked immunosorbent assay (ELISA) kits. The SMB+MSC sheets secreted significantly more HGF and VEGF than the SMB-only sheets. $N=5$ in each group. $^{*}p<0.05$. G-CSF, granulocyte-colony stimulating factor; HGF, hepatocyte growth factor; IL, interleukin; PDGF, platelet-derived growth factor; PECAM, platelet/endothelial cell adhesion molecule; VEGF, vascular endothelial growth factor. Error bars=SD.

infarction (MI), FS, EF, and anterior wall thickness showed steady reductions, whereas EDD/ESD showed steady increases, suggesting progressive LV remodeling.

Following either SMB-only or MSC-only cell-sheet transplantation, the heart showed mild recovery, including increases in FS, EF, and anterior wall thickness. At 2, 4, 6, and 8 weeks after treatment, FS, EF, and anterior wall thickness were significantly greater following SMB-only or MSC-only cell-sheet transplantation than the control, and significantly better recovery was obtained using the co-cultured cell sheets than either single cell-type sheet (Fig. 3A).

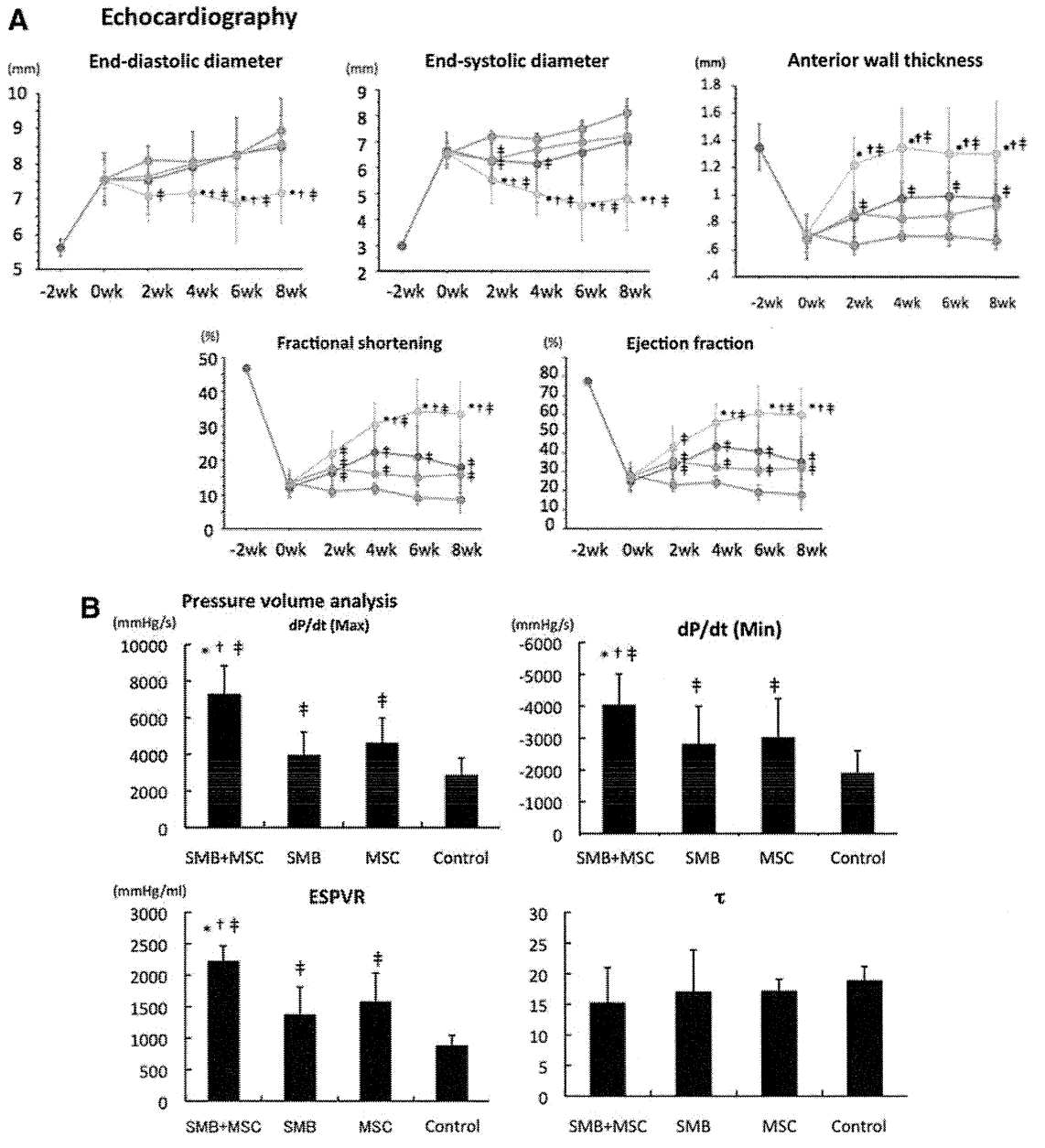

FIG. 3. Cardiac functional recovery after cell-sheet transplantation. **(A)** Echocardiographic analysis. Fractional shortening, ejection fraction, and anterior wall thickness were significantly improved 2, 4, 6, and 8 weeks after cell-sheet transplantation in the SMB+MSC sheet group, compared with the other three groups. Left ventricular end-diastolic and end-systolic diameters in the SMB+MSC sheet group were significantly decreased 4, 6, and 8 weeks after cell-sheet transplantation, compared with the other three groups ($N=10$ in each group. SMB+MSC group, green line; SMB group, blue line; MSC group, pink line; control group, red line). **(B)** Hemodynamic measurements determined by cardiac catheterization ($n=10$ in each group). Max. and min. dP/dt and ESPVR significantly improved in the SMB+MSC group, compared with the other three groups. Max. dP/dt, maximal rate of change in left ventricular pressure; min. dP/dt, minimal rate of change in left ventricular pressure; ESPVR, end-systolic pressure-volume relationship; EDPVR, end-diastolic pressure-volume relationship; τ, active part of relaxation shown by the relaxation time constant. $N=10$ in each group. $^{*}p<0.05$ versus SMB-only cell sheet. $^{\dagger}p<0.05$ versus MSC-only cell sheet. $^{\ddagger}p<0.05$ versus control. n.s., not significant. Error bars=SD. Color images available online at www.liebertpub.com/tea

Assessment by LV catheter showed a similar trend. Eight weeks after transplantation, the maximal and minimal rate of change in LV pressure (max. dP/dt and min. dP/dt, respectively) and end-systolic pressure-volume relationship (ESPVR) were significantly greater following either single-cell-type cell-sheet transplantation than the control, but τ was significantly different. After the co-culture cell-sheet transplantation, the max. dP/dt, min. dP/dt, and ESPVR improved further, with no significant difference in EDPVR or τ (Fig. 3B).

Reverse remodeling after co-culture cell-sheet transplantation

The LV structure was better maintained after SMB-only or MSC-only cell-sheet transplantation, compared to the control, in which the LV cavity was severely enlarged with a thin anterior wall, as assessed by HE staining (Fig. 4A). The LV structure was even better maintained after the co-culture cell-sheet transplantation. In the control, abundant collagen accumulations were observed in the infarct area, and diffuse fibrotic changes were induced in the remote area, whereas collagen accumulation was attenuated in both the remote area with the single cell-type sheet transplants, as assessed by Masson's trichrome staining (Fig. 4B, C). Fibrotic changes in the remote area were further attenuated by transplantation of the co-cultured cell sheet (Fig. 4D).

A greater number of vWF-positive blood vessels was detected in the peri-infarcted myocardium following the transplantation of either single-cell-type cell sheet, compared to the control (Fig. 5A), and even more vWF-positive blood vessels were seen with transplantation of the co-cultured cell sheet. The capillary density in the peri-infarcted myocardium, which was semi-quantitatively assessed in 10 randomly selected individual fields, was significantly greater following the transplantation of either single-cell-type cell sheet, compared to the control (Fig. 5B), and it was further increased after the co-cultured cell-sheet transplantation.

Major intercellular signaling molecules relevant to angiogenesis and cell survival were analyzed by western blotting. The ratio of p-STAT3 over total STAT3 was greatly increased after co-cultured cell-sheet transplantation (Fig. 5C).

Survival of transplanted cells in the heart

Four weeks after the cell-sheet transplantation, significantly more transplanted rat cells survived in co-cultured sheets than SMB-only sheets, as analyzed by PCR assays for the Y-chromosome-specific *Sry* gene (Fig. 6A).

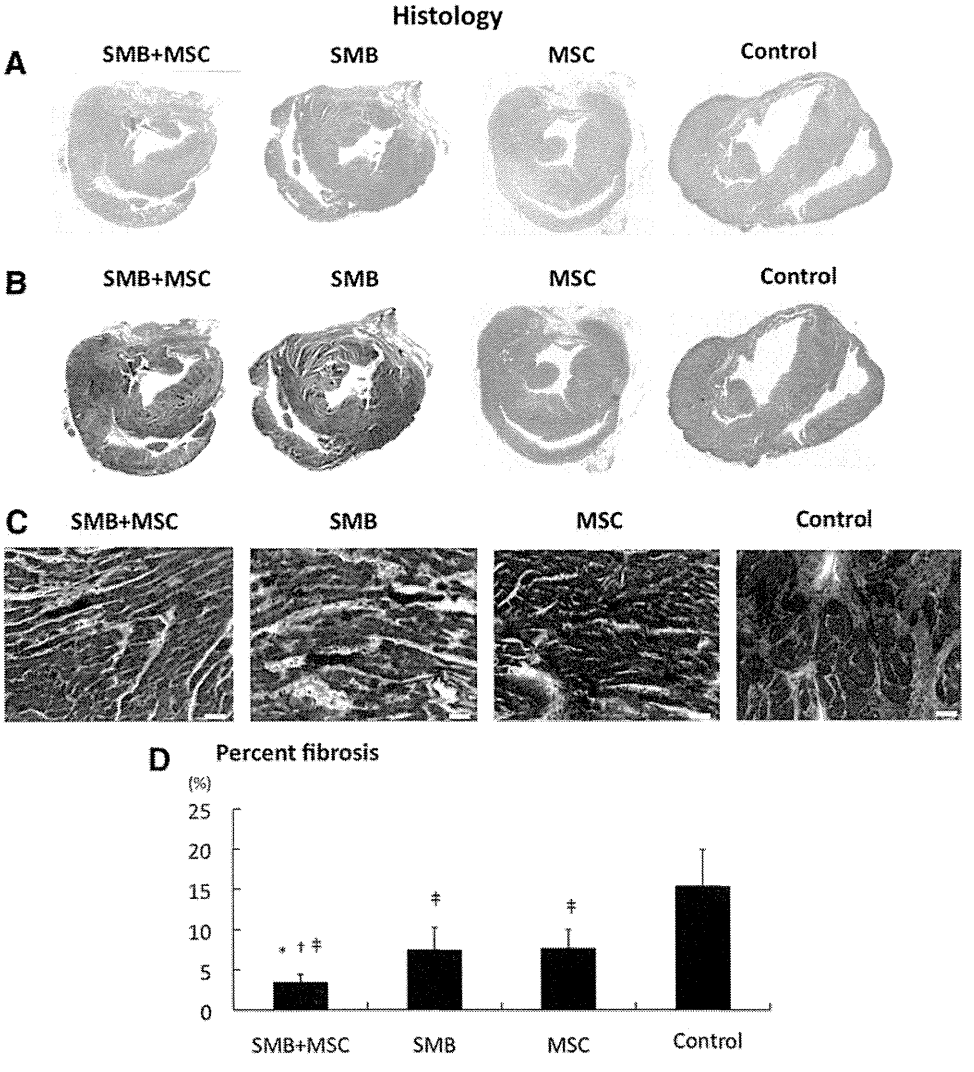

FIG. 4. Histological reverse remodeling after cell-sheet transplantation. **(A)** Macroscopic (×40) views of the heart stained by hematoxylin–eosin. **(B)** Macroscopic (×40) views of the heart stained by Masson's trichrome. **(C)** Microscopic (×200) representative Masson's trichrome staining at the remote myocardium (white bar = 40 μm). **(D)** Quantification of percent fibrosis at the remote area. Significant suppression of fibrosis was found after SMB + MSC sheet transplantation compared with the other three groups. $N = 5$ in each group. $^{*}p < 0.05$ versus SMB. $^{\dagger}p < 0.05$ versus MSC. $^{\ddagger}p < 0.05$ versus control. Error bars = SD. Color images available online at www.liebertpub.com/tea

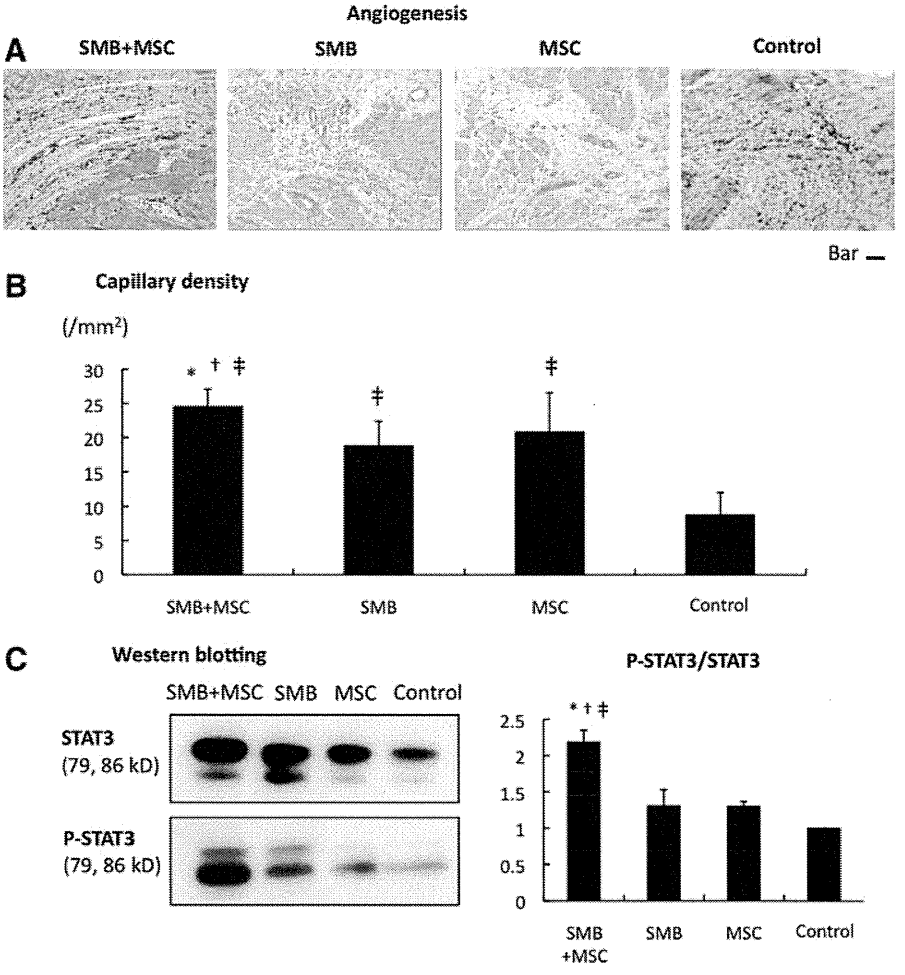

FIG. 5. Angiogenesis. **(A)** Microscopic (×100) views of sections of the peri-infarct border-zone region stained with anti-von Willebrand factor antibody (factor VIII) in the four groups (bar = 50 μm). **(B)** Capillary density: the SMB + MSC group showed significant improvement in capillary density as assessed by immunostaining for von-Willebrand factor-positive blood vessels. $N = 5$ in each group. **(C)** Western blotting showing enhanced STAT3 phosphorylation over total STAT3 in the SMB + MSC sheet group. $N = 3$ in each group. $^{*}p < 0.05$ versus SMB. $^{\dagger}p < 0.05$ versus MSC. $^{\ddagger}p < 0.05$ versus control. Error bars = SD. STAT3, signal transducer and activator of transcription 3. Color images available online at www.liebertpub.com/tea

The percentage of TUNEL-positive myocytes was significantly lower following the transplantation of the co-cultured cell sheet compared to the control (Fig. 6B).

Akt-1 and Bcl-2 were highly expressed in the heart following transplantation of the SMB-only or co-cultured cell sheet, compared with the control, as analyzed by real-time quantitative PCR using rat-specific primers (Fig. 6C).

Notably, among apoptosis-signaling molecules, Bcl_2 and cleaved PARP were increased 1 day after the co-culture cell-sheet transplantation. There was no significant difference in the ratio of phosphorylation of Akt over Akt (Fig. 6D).

Upregulation of cardioprotective factors in the myocardium after cell-sheet transplantation

The mRNA expression of cardioprotective factors, such as HGF, VEGF, IGF-1, and bFGF, in the infarct and infarct-remote areas of the myocardium was analyzed by real-time PCR using rat-specific primers, which detected factors released by transplanted SMB or the native myocardium. The expression of these factors was not significantly different after transplantation of either single-cell-type cell sheet or no treatment, except for HGF expression in the infarct area, which was significantly greater after the SMB-only sheet transplantation (Fig. 7A, B). In contrast, following transplantation of the co-cultured cell sheet, the HGF and VEGF levels in the infarct area were significantly greater than after transplantation of either single cell-type cell sheet or control, although the levels of IGF-1 and bFGF were unchanged (Fig. 2A). The intramyocardial protein levels of HGF and VEGF, analyzed by ELISA, were significantly greater after transplantation of the co-cultured cell sheet than of either single-cell-type cell sheet or no treatment (Fig. 7C).

Immunoconfocal microscopy showed that HGF was found in the transplanted SMBs from the co-cultured cell sheet (Fig. 8A).

MSCs differentiate into new vessels in situ

The differentiation capacity of the transplanted h-MSCs was assessed by immunoconfocal microscopy. As expected, no human-derived cells were seen in either the r-SMB-only transplantation group or the control group. However, human vWF-positive staining was observed in the host vessels in both the co-cultured cell-sheet group and the h-MSC-only cell-sheet transplantation group. Thus, the h-MSCs could differentiate into vessel walls *in vivo* (Fig. 8B).

Discussion

Here, we demonstrated that SMB cell sheets abundantly synthesized and extracellularly released multiple cytokines and chemokines, and adding MSCs enhanced the SMB cell

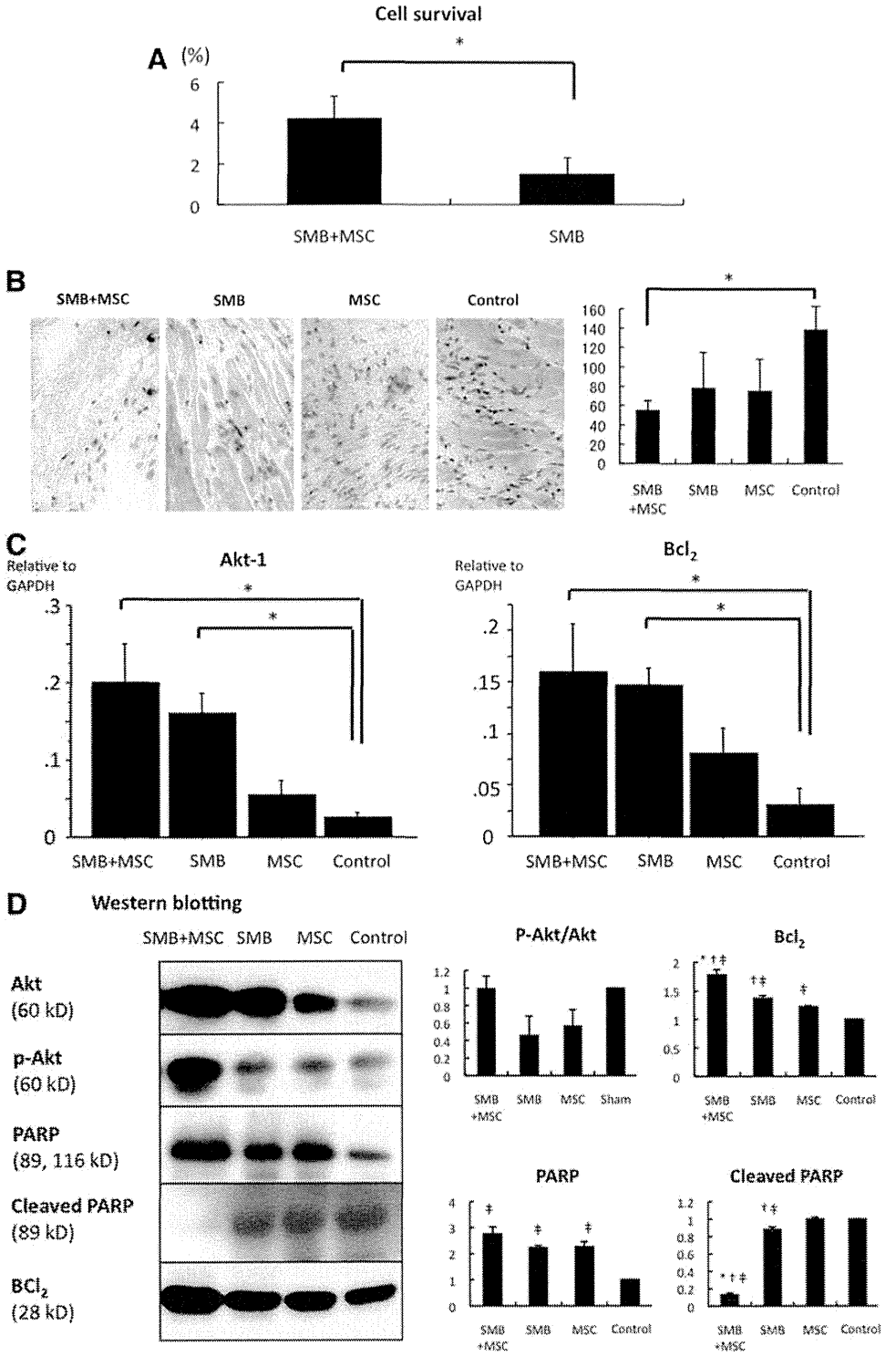

FIG. 6. Cell survival. **(A)** Survival of transplanted cells of rat origin was significantly greater in the SMB+MSC sheet group than in the SMB sheet group. $N = 4$ in each group. $^*p < 0.05$. **(B)** The number of terminal deoxynucleotidyl transferase-mediated dUTP nick end labeling (TUNEL)-positive myocytes was significantly lower in SMB+MSC group than in control. $N = 4$ in each group. $^*p < 0.05$. **(C)** Expressions of mRNA in the transplanted infarct area of hearts were determined by real-time PCR using rat-specific primers. The expressions of Akt-1 and Bcl_2 mRNA were significantly increased in the SMB+MSC sheet group compared with the other groups. $N = 4$ in each group. $^*p < 0.05$. **(D)** Western blotting showed that Bcl_2 was much more enhanced, and cleaved PARP was significantly downregulated in the SMB+MSC group. There was no significant difference in the ratio of phosphorylation of Akt over Akt. $N = 3$ in each group. $^*p < 0.05$ versus SMB. $^\dagger p < 0.05$ versus MSC. $^\ddagger p < 0.05$ versus control. Error bars = SD. Color images available online at www.liebertpub.com/tea

sheets' release of HGF and VEGF but not of IGF-1, bFGF, or SDF-1, *in vitro*. The transplantation of SMB-only cell sheets into the chronically ischemic failing rat heart resulted in reversed LV remodeling, including increased capillaries, attenuated collagen accumulation, and prolonged cell survival, which increased global functional recovery, mediated by the paracrine effects of upregulated HGF and VEGF in the myocardium.

Recent studies, including ours,[3–9] have suggested that a paracrine effect mediated by cytokines secreted from the transplanted cell sheets is a likely mechanism for the therapeutic effects on the myocardium, which was a focus of the present study. Here, we added h-MSCs to the cell sheets to enhance the potential performance of the transplanted r-SMB sheets. Our *in vitro* findings, that h-MSCs enhanced rat mRNA levels and the secretion of cytokines such as r-HGF

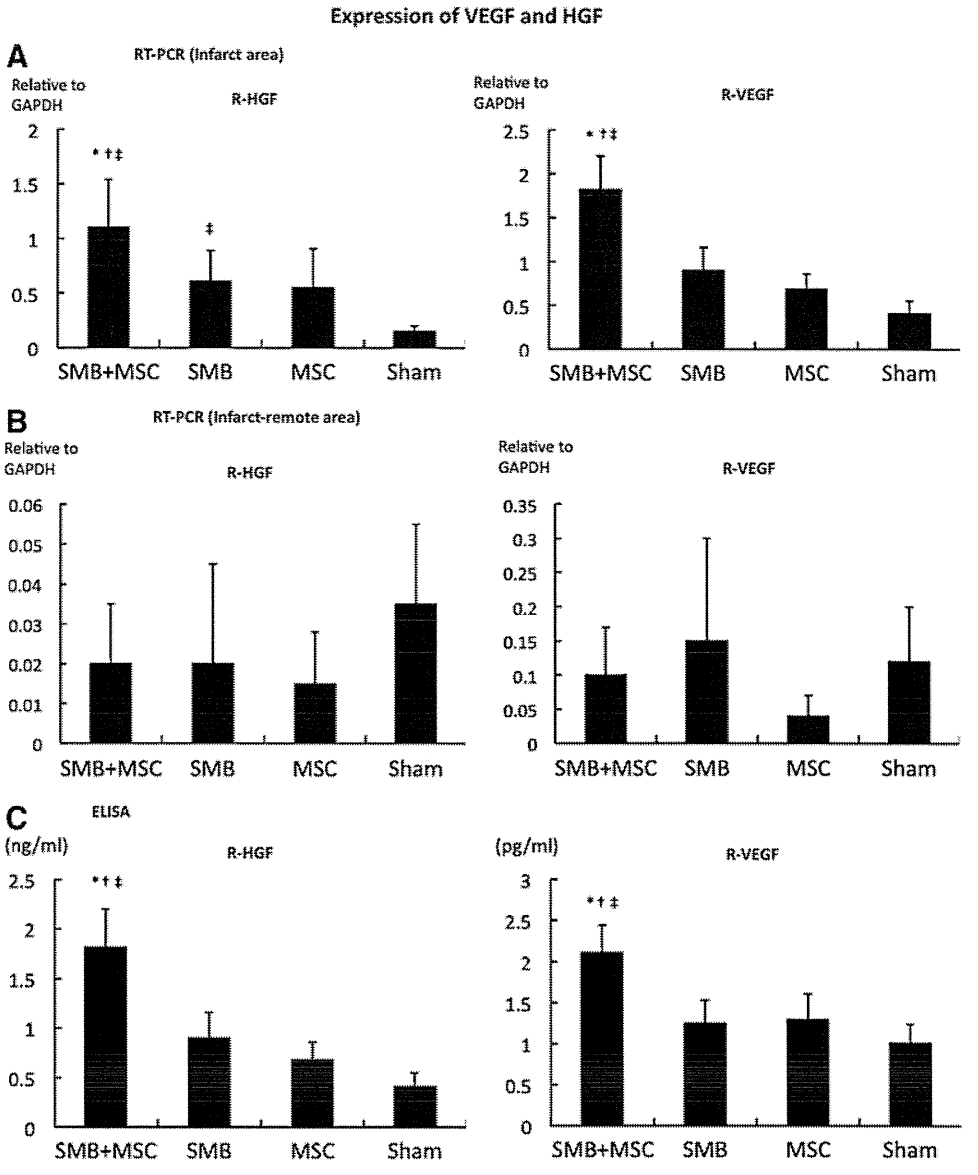

FIG. 7. Expression of VEGF and HGF is higher at the infarct area. **(A, B)** Levels of mRNA in the transplanted infarct and infarct-remote heart areas by real-time PCR using rat-specific primers. The HGF and VEGF mRNA expressions within the transplanted infarct area of the hearts were significantly increased in the SMB + MSC sheet group compared with the other groups. $N = 4$ in each group. $^{*}p < 0.05$ versus SMB. $^{\dagger}p < 0.05$ versus MSC. $^{\ddagger}p < 0.05$ versus sham. **(C)** Intramyocardial protein levels of HGF and VEGF, analyzed by ELISA, were significantly greater in the heart in the SMB + MSC sheet group compared with the other groups. $^{*}p < 0.05$ versus SMB. $^{\dagger}p < 0.05$ versus MSC. $^{\ddagger}p < 0.05$ versus control. Error bars = SD.

and r-VEGF from r-SMBs, suggested that transplanted co-cultured cell sheets would secrete r-HGF and r-VEGF *in vivo*. Although the exact mechanisms by which "feeder layers" support cell growth have not been elucidated, it is possible that h-MSCs enhance the r-SMBs directly (via cellular interaction) or indirectly (via secreted cytokines from the h-MSCs).[16] A more comprehensive examination aimed at differentiating these effects might help reveal how feeder layers work.

HGF and VEGF participate in many complex molecular and cellular mechanisms, and their signaling pathways have been intensively investigated *in vivo*.[3,9] SMBs or MSCs act as the natural supplier of both HGF and VEGF and provide feasible and safe sources for cell therapy in clinical applications. Indeed, SMBs and bone marrow-derived mesenchymal stem cell sheets can secrete growth factors (e.g., HGF and VEGF) into the myocardium and accelerate neovascularization in the damaged area.[5–8] More recent reports have revealed that angiogenesis induced by HGF or VEGF, an antifibrotic effect promoted by HGF, or the migration and survival of SMBs supported by VEGF,[17] could be beneficial to an impaired heart.[7,8] In addition, our data from a cytokine/chemokine multiplex immunology assay indicate that leptin may also be beneficial (e.g., by inducing angiogenesis though the Jak/STAT pathway).[18] Other cytokines may also contribute to the improvement of cardiac function by single-cell-type cell sheets in as-yet-undiscovered ways.

The mechanism by which the implanted cell sheet attenuates ventricular remodeling and improves cardiac function seems to depend on the cell sheet being placed over the scarred area of the myocardium and leads to repair of the anterior wall thickness, reduction of LV wall stress, and the improvement of ejection performance.[3] Previous studies indicated that the surviving myocardium and implanted cell sheet attenuate complex cellular and molecular events, including hypertrophy, fibrosis, apoptosis of the myocardium, and the pathological accumulation of extracellular matrix.[9] Similarly, the greater cellularity observed after cell-sheet

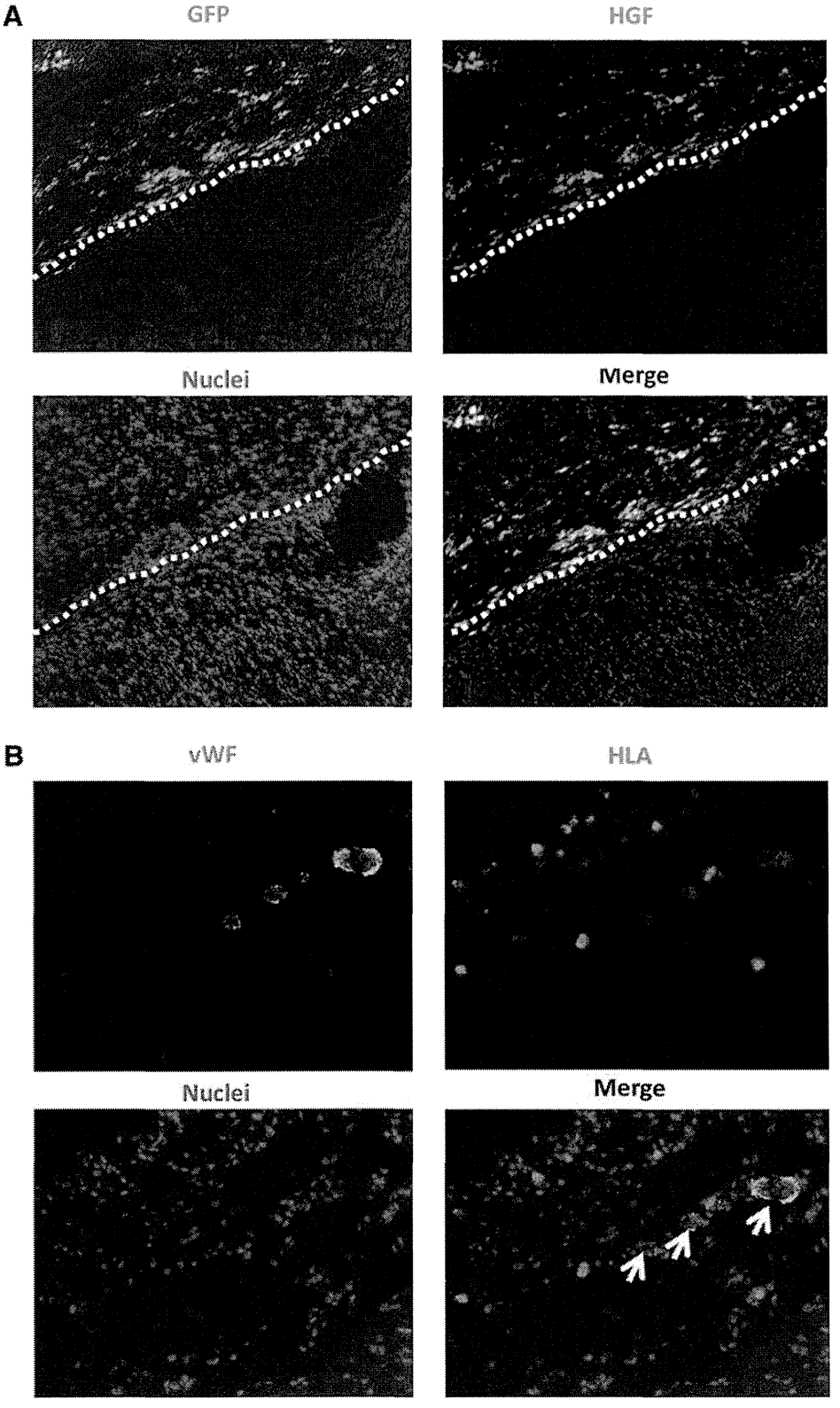

FIG. 8. Characterization of transplanted cells. **(A)** Cryosections were stained with an antibody to HGF to detect the distribution of SMB and HGF in the heart. HGF expressions and GFP-positive cells were found in the myocardium after transplantation of the SMB + MSC sheet. White broken line shows the border between the transplanted cell sheet and the host heart. Green indicates GFP; red, HGF; blue, nuclei. **(B)** Cryosections were stained with antibodies to human leukocyte antigen (HLA) and to von Willebrand factor (vWF). Human vWF-positive (white arrows) staining was observed in the host vessels in the h-MSC-transplanted group. Green indicates vWF; red, HLA; blue, nuclei. Color images available online at www.liebertpub.com/tea

treatment might have resulted from released SDF-1, which is related to cell migration, adhesion, and proliferation, by the transplanted cell sheet[19,20]

In this study, we performed additional investigations on the paracrine mechanism from a new perspective, by analyzing signaling pathways within the myocardium following cell-sheet transplantation because the signals induced by released paracrine mediators presumably activate phosphorylation cascades of signaling molecules. We found that STAT3 and Akt phosphorylations were significantly increased, and cleaved PARP was significantly downregulated, 24 h after the co-cultured cell-sheet implantation. Together

with our findings that vascular density was significantly enhanced, and myocardial apoptosis and fibrosis was significantly attenuated in the co-cultured group, it is possible that the co-cultured cell-sheet transplantation induced angiogenesis partially through the Jak/STAT signaling pathway[18] and that it prolonged cell survival by preventing apoptosis through PI-3K/Akt-mediated signaling, which is partially modulated by HGF.[21]

Although we emphasized combining SMBs with h-MSCs, some investigators have focused on different combinations of various cell sources. Sekine *et al.*[22] reported that cardiomyocytes co-cultured with endothelial cells induce greater numbers of capillaries, due to increased secretion of angiogenic growth factors.[22] Another report showed that a dermal fibroblast sheet co-cultured with endothelial progenitor cells was more effective than either single cell-type sheet for improving damaged heart function, accompanied by the inhibition of fibrotic tissue formation and the acceleration of neovascularization in the infarcted myocardium.[23] Thus, the paracrine effect may be improved by combining different cell sources; however, further investigation focused on determining the optimal combinations of cell sources is needed.

Regarding h-MSCs as a cell source, bone marrow-derived or adipose tissue-derived stem cells are reported to differentiate into mature endothelial cells and participate in blood vessel formation in the recipient heart.[24] The presence of endothelial capillary networks improves the survival and organization of implanted cells by maintaining a minimum intercapillary distance to provide oxygen and nutrients. Therefore, the presence of endothelial capillary networks may be partially correlated with cardiac function.

For future tissue engineering for cardiac therapy, the creation of thick cell-dense constructs with functional vessels may be essential. Capillary formation occurs via two basic vessel-constructing processes: angiogenesis, that is, the formation of new capillaries via sprouting or intussusception from pre-existing vessels, and vasculogenesis, which occurs in the developing embryo.[25] Here, the morphology of the vessel formation within myocardial tissues, including the diameter, composition, and fragility of vessel walls, suggested that improper vascularization may occur under pathological conditions. It is likely that not only biological factors but also physical stimuli such as flow and shear stress are required to mimic the *in vivo* environment and enable the formation of mature vascular networks.

A potential limitation of this study is that the exact number of transplanted cells was different in each group *in vivo*. Clinically, open-chest surgery is unlikely to gain easy acceptance except in certain situations; however, less invasive methods (e.g., intracoronary catheter-based procedures) might be technically difficult for carefully placing the cell sheets. Additionally, further studies that include longer timeframe than 8 weeks are needed to examine a longer term restoration of heart function post-MI. It is likely that the source of HGF is the transplanted SMB; however, it is unclear whether the source of other therapeutic cytokines is the transplanted cells, such as SMBs, MSCs, or both, or native cardiac cells.

In conclusion, we found that h-MSCs enhanced the paracrine effects of r-SMB sheets, thus enhancing angiogenesis, lowering fibrosis, inhibiting cellular hypertrophy, improving cardiac function, and prolonging cell survival in MI model rats. These observations of improved effects from this co-cultured cell sheet may lead to new regeneration therapies for heart failure following advanced cardiomyopathy that are superior to the conventional SMB-only cell-sheet technique.

Acknowledgments

We thank Dr. Eiji Kobayashi and Takashi Murakami for kindly providing the GFP transgenic Lewis rats. We thank Mr. Akima Harada, Mr. Shigeru Matsumi, and Mrs. Masako Yokoyama for their excellent technical assistance.

Sources of Funding: This study was supported by Grants for the Research and Development of the Myocardial Regeneration Medicine Program from the New Energy Industrial Technology Development Organization (NEDO), Japan. This research was supported by the Health and Labour Sciences Research Grants, Research on intractable diseases.

Disclosure Statement

T.S. is a consultant for CellSeed, Inc. T.O. is an Advisory Board Member in CellSeed, Inc., and the inventor/developer designated on the patent for temperature-responsive culture surfaces.

References

1. Menasche, P., Hagege, A.A., Scorsin, M., Puzet, B., Desnos, B., Schwartz, K., Vilquin, J.T., and Marolleau, J.P. Myoblast transplantation in heart failure. Lancet **357,** 279, 2001.
2. Hagege, A.A., Marolleau, J.P., Vilqiun, J.T., Alheritiere, A., Peyrard, S., Duboc, D., Abergel, E., Messas, E., Mousseaux, E., Schwartz, K., Desnos, M., and Menasche, P. Skeletal myoblast transplantation in ischemic heart failure: Long-term follow-up of the first phase I cohort of patients. Circulation **114,** I108, 2006.
3. Miyagawa, S., Roth, M., Saito, A., Sawa, Y., and Kostin, S. Tissue-engineered cardiac constructs for cardiac repair. Ann Thorac Surg **91,** 320, 2011.
4. Imanishi, Y., Miyagawa, S., Maeda, N., Fukushima, S., Kitagawa-Sakakida, S., Daimon, T., Hirata, A., Shimizu, T., Okano, T., Shimomura, I., and Sawa, Y. Induced adipocyte cell-sheet ameliorates cardiac dysfunction in a mouse myocardial infarction model: a novel drug delivery system for heart failure. Circulation **124,** S10, 2011.
5. Miyagawa, S., Saito, A., Sakaguchi, T., Yoshikawa, Y., Yamauchi, T., Imanishi, Y., Kawaguchi, N., Teramoto, N., Matsuura, N., Iida, H., Shimizu, T., Okano, T., and Sawa, Y. Impaired myocardium regeneration with skeletal cell sheets—a preclinical trial for tissue-engineered regeneration therapy. Transplantation **90,** 364, 2010.
6. Fujita, T., Sakaguchi, T., Miyagawa, S., Saito, A., Sekiya, N., Izutani, H., and Sawa, Y. Clinical impact of combined transplantation of autologous skeletal myoblasts and bone marrow mononuclear cells in patients with severely deteriorated ischemic cardiomyopathy. Surg Today **41,** 1029, 2011.
7. Sekiya, N., Matsumiya, G., Miyagawa, S., Saito, A., Shimizu, T., Okano, T., Kawaguchi, N., Matsuura, N., and Sawa, Y. Layered implantation of myoblast sheets attenuates adverse cardiac remodeling of the infarcted heart. J Thorac Cardiovasc Surg **138,** 985, 2009.
8. Memon, I.A., Sawa, Y., Fukushima, N., Matsumiya, G., Miyagawa, S., Taketani, S., Sakakida, S.K., Kondoh, H.,

Aleshin, A.N., Shimizu, T., Okano, T., and Matsuda, H. Repair of impaired myocardium by means of implantation of engineered autologous myoblast sheets. J Thorac Cardiovasc Surg **130,** 646, 2009.
9. Matuura, K., Honda, A., Nagai, T., Fukushima, N., Iwanaga, K., Tokunaga, M., Shimizu, T., Okano, T., Kasanuki, H., Hagiwara, N., and Komuro, I. Transplantation of cardiac progenitor cells ameliorates cardiac dysfunction after myocardial infarction in mice. J Clin Invest **119,** 2204, 2009.
10. Majumdar, M.K., Thiede, M.A., Mosca, J.D., Moorman, M., and Gerson, S.L. Phenotypic and functional comparison of cultures of marrow-derived mesenchymal stem cells (MSCs) and stromal cells. J Cell Physiol **176,** 57, 1998.
11. Richards, M., Fong, C.Y., Chan, W.K., Wong, P.C., and Bongso, A. Human feeders support prolonged undifferentiated growth of human inner cell masses and embryonic stem cells. Nat Biotechnol **20,** 933, 2002.
12. Ohkura, H., Matsuyama, A., Lee, C.M., Saga, A., Kakuta-Yamamoto, A., Nagao, A., Sougawa, N., Sekiya, N., Takekita, K., Shudo, Y., Miyagawa, S., Komoda, H., Okano, T., and Sawa, Y. Cardiomyoblast-like cells differentiated from human adipose tissue-derived mesenchymal stem cells improve left ventricular dysfunction and survival in a rat myocardial infarction model. Tissue Eng Part C Methods **16,** 417, 2010.
13. Pittenger, M.F., Mackay, A.M., Beck, S.C., Jaiswal, R.K., Douglas, R., Mosca, J.D., Moorman, M.A., Simonetti, D.W., Craig, S., and Marshak, D.R. Multilineage potential of adult human mesenchymal stem cells. Science **284,** 143, 1999.
14. Jiang, Y., Jahagirar, B.N., Reinhardt, R.L., Schwartz, R.E., Keene, C.D., Ortiz-Gonzales, X.R., Reyes, M., Lenrik, T., Lund, T., Blackstad, M., Du, J., Aldrich, S., Lisberg, A., Low, W.C., Largaespada, D.A., and Vertaille, C.M. Pluripotency of mesenchymal stem cells derived from adult marrow. Nature **418,** 41, 2002.
15. Inoue, H., Ohsawa, I., Murakami, T., Kimura, A., Hakamata, Y., Sato, Y., Kaneko, T., Takahashi, M., Okada, T., Ozawa, K., Francis, J., Leone, P., and Kobayashi, E. Development of new inbred transgenic strains of rats with LacZ or GFP. Biochem Biophys Res Commun **329,** 288, 2005.
16. Kirouac Dc, and Zandstra, P.W. Understanding cellular networks to improve hematopoietic stem cell expansion cultures. Curr Opin Biotechnol **17,** 538, 2006.
17. Germani, A., Di Carlo, A., Mangoni, A., Straino, S., Giacinti, C., Turrini, P., Biglioli, P., and Capogrosse, M.C. Vascular endothelial growth factor modulates skeletal myoblast function. Am J Pathol **163,** 1417, 2003.
18. Sierra-Honigmann, M.R., Nath, A.K., Murakami, C., García-Cardeña, G., Papapetropoulos, A., Sessa, W.C., Madge, L.A., Schechner, J.S., Schwabb, M.B., Polverini, P.J., and Flores-Riveros, J.R. Biological action of leptin as an angiogenic factor. Science **281,** 1683, 1998.
19. Hiesinger, W., Perez-Aguilar, J.M., Atluri, P., Marotta, N.A., Frederick, J.R., Fitzpatrick, J.R., 3rd, McCormick, R.C., Muenzer, J.R., Yang, E.C., Levit, R.D., Yuan, L.J., Macarthur, J.W., Saven, J.G., and Woo, Y.J. Computational protein design to reengineer stromal cell-derived factor-1a generates an effective and translatable angiogenic polypeptide analog. Circulation **124,** S18, 2011.
20. Frederick, J.R., Fitzpatrick, J.R., 3rd, McCormick, R.C., Harris, D.A., Kim, A.Y., Muenzer, J.R., Marotta, N., Smith, M.J., Cohen, J.E., Hiesinger, W., Atluri, P., and Woo, Y.J. Stromal cell-derived factor-1alpha activation of tissue-engineered endothelial progenitor cell matrix enhances ventricular function after myocardial infarction by inducing neovasculogenesis. Circulation **122,** S107, 2010.
21. Kakazu, A., Chandrasekher, G., and Bazan, H.E. HGF protects corneal epithelial cells from apoptosis by the PI-3K/Akt-1/Bad- but not the ERK 1/2-mediated signaling pathway. Invest Ophthalmol Vis Sci **45,** 3485, 2004.
22. Sekine, H., Shimizu, T., Hobo, K., Sekiya, S., Yang, J., Yamato, M., Kurosawa, H., Kobayashi, E., and Okano, T. Endothelial cell coculture within tissue-engineered cardiomyocyte sheets enhances neovascularization and improve cardiac function of ischemic hearts. Circulation **118,** S145, 2008.
23. Kobayashi, H., Shimizu, T., Yamato, M., Tono, K., Masuda, H., Asahara, T., Kasanuki, H., and Okano, T. Fibroblast sheets co-cultured with endothelial progenitor cells improve cardiac function of infarcted hearts. J Artif Organs **11,** 141, 2008.
24. Miyahara, Y., Nagaya, N., Kataoka, M., Yanagawa, B., Tanaka, K., Hao, H., Ishino, K., Ishida, H., Shimizu, T., Kangawa, K., Sano, S., Okano, T., Kitamura, S., and Mori, H. Monolayered mesenchymal stem cells repair scarred myocardium after myocardial infarction. Nat Med **12,** 459, 2006.
25. Risau, W. Mechanisms of angiogenesis. Nature **386,** 671, 1997.

Address correspondence to:
Yoshiki Sawa, MD, PhD
Department of Cardiovascular Surgery
Osaka University Graduate School of Medicine
Suita
Osaka 565-0871
Japan

E-mail: sawa-p@surg1.med.osaka-u.ac.jp

Received: September 2, 2012
Accepted: September 25, 2013
Online Publication Date: December 31, 2013